10. Yu. B. Kolesnikov and A. B. Tsinober, "Experimental study of two-dimensional turbulence behind a grid," Izv. Akad. Nauk SSSR, Mekh. Zhidk. Gaza, No. 4 (1974).
11. J. Sommeria and R. Moreau, "Why, how, and when MHD-turbulence becomes two-dimensional," J. Fluid Mech., 118 (1982).
12. Y. Couder, "Two-dimensional grid turbulence in a thin liquid film," J. Phys. (Paris) Lett., 45, No. 8 (1984).
13. D. V. Lyubimov, G. F. Putin, and V. I. Chernatynskii, "Convective motions in a Hele-Shaw cell," Dokl. Akad. Nauk SSSR, 235, No. 3 (1977).
14. A. L. Tseskis, "Two-dimensional turbulence," Zh. Eksp. Teor. Fiz., 83, No. 1 (1982).
15. G. P. Bogatyrev, V. G. Gilev, and V. D. Zimin, "Space-time spectra of stochastic oscillations in a convection cell," Pis'ma Zh. Eksp. Teor. Fiz., 32, No. 3 (1980).
16. V. A. Barannikov, G. P. Bogatyrev, V. D. Zimin, A. I. Ketov, and V. G. Shaidurov, "Laws of alternation of peaks in spectra of stochastic oscillations of hydrodynamic systems," Preprint Inst. Mekh. Sploshnykh Sred UNTs Akad. Nauk SSSR (1982).

MODELING TURBULENT TRANSFER IN A CHANNEL BY MEANS OF POINT VORTICES

P. I. Geshev and B. S. Ezdin

UDC 532.527+532.4

Much attention has recently been paid to the direct numerical modeling of turbulence. Some studies have examined three-dimensional turbulent flow in a channel at moderate Reynolds numbers Re by numerically solving the complete system of Navier–Stokes equations [1]. The main difficulty in such calculations is that motions on a scale much smaller than the distance between the nodes of the finest computing grids used in practice are important in turbulence at sufficiently large Re. Despite the increasing capacity of modern computers, the limitation on Re remains. There are other approaches to the numerical modeling of wall turbulence, such as the method of large vortices [2]. In this method, the scales of motion are divided into a calculable part (by means of "filtered" Navier–Stokes equations for large scales) and a closable, small-scale part (a one-parameter closing relation is generally used), i.e., the hypothesis of the independence of small-scale motions from large-scale motions is employed. In accordance with the principle of the similarity of turbulent flows with respect to the Reynolds number [3], the large-scale motion of a continuum away from the walls is slightly dependent on Re. Thus, it can be described by the equations of an ideal swirled fluid. In the proposed computational scheme, transverse motion is modeled by the inviscid two-dimensional motion of point vortices, while the complete Navier–Stokes equation, with a constant pressure gradient, is calculated in the mean direction of motion. Two-dimensional point vortices have been used to study mainly free flows – jets and wakes in flow about different recesses and projections. It was shown in [4] that the spectral energy flux is constant in a system of point vortices and the flow spectrum is close to a Kolmogorov spectrum. The "5/3" law follows from similarity theory in the case of isotropic turbulence. In wall turbulence, this theory leads to logarithmic velocity profiles in the region where the flow of the longitudinal component of momentum to the wall is constant [5]. Considering the successful modeling of isotropic turbulence in [4], there is hope for obtaining interesting results in wall turbulence by modeling turbulent transfer by the method of longitudinal point vortices. It was shown in the present study that such calculations give results which agree qualitatively with experimental findings; the logarithmic profiles of velocity and temperature are calculated, profiles of the Reynolds stresses and turbulent heat fluxes are obtained, and the amplitudes of fluctuating quantities are investigated. A model of turbulence based on point vortices should be considered a direct numerical model. Such an approach has an undoubted advantage, since it does not require any closing assumptions.

Novosibirsk. Translated from Zhurnal Prikladnoi Mekhaniki i Tekhnicheskoi Fiziki, No. 2, pp. 79-84, March-April, 1986. Original article submitted February 6, 1985.

0021-8944/86/2702-0228 $12.50

1. Formulation of the Problem. We will examine the turbulent flow of an incompressible liquid flowing in a plane channel of height H in the direction of the x axis. The y axis is directed normal to the walls, while the z axis is normal to the x and y axes, i.e., the channel forms two planes y = 0 and y = H. The flow is assumed to be uniform along the channel (along the x axis) – the longitudinal velocity depends only on the transverse coordinates y and z and the time t; its mean characteristics are also independent of z, which is very important and is used to obtain large statistical samples. A system of 10^3-10^4 point vortices is used to model motions in the y and z directions. The longitudinal velocity u and temperature θ are determined by solving the equations of convective transfer of momentum and heat, respectively.

We introduce the dimensionless variables (the dimensional variables have the superscript 0):

$$x = x^0/H,\ y = y^0/H,\ z = z^0/H,$$
$$v = v^0/v^*,\ p = p^0/(\rho v^{*2}),\ \Theta = (T - T_w)/\Theta^*,$$

where $v^* = \sqrt{\tau_w/\rho}$ is the dynamic velocity; τ_w, shear stress on the wall; ρ, density of the liquid; $\Theta^* = q_w/(\rho c_p v^*)$, dynamic temperature; q_w, heat flux from the wall; c_p, specific heat of the liquid. The system of two-dimensional nonsteady equations is written as follows in the new variables:

$$\Delta\psi = -\omega; \tag{1.1}$$

$$\frac{\partial u}{\partial t} + v\frac{\partial u}{\partial y} + w\frac{\partial u}{\partial z} = -\frac{dp}{dx} + \frac{1}{\mathrm{Re}^*}\left(\frac{\partial^2 u}{\partial y^2} + \frac{\partial^2 u}{\partial z^2}\right); \tag{1.2}$$

$$\frac{\partial \Theta}{\partial t} + v\frac{\partial \Theta}{\partial y} + w\frac{\partial \Theta}{\partial z} = \frac{1}{\mathrm{Pe}^*}\left(\frac{\partial^2 \Theta}{\partial y^2} + \frac{\partial^2 \Theta}{\partial z^2}\right), \tag{1.3}$$

where $\mathrm{Re}^* = Hv^*/\nu$; $\mathrm{Pe}^* = Hv^*/a$; ν is viscosity; a is the diffusivity of the liquid. The components of velocity, the stream function ψ, and vorticity ω are connected by the relation $w = \partial\psi/\partial y$, $v = -\partial\psi/\partial z$, $\omega = \mathrm{rot}\,\mathbf{u}$. For discrete ideal vortices, all of the vorticity is assumed to be concentrated at individual points:

$$\omega = \sum_{n=1}^{N} \Gamma_n \delta(\mathbf{x} - \mathbf{x}_n(t)). \tag{1.4}$$

Here, Γ_n is the circulation around the n-th vortex; δ is the delta function; $x_n(t)$ is the instantaneous position of the n-th vortex.

The boundary conditions with respect to the variable y:

for nonflow condition

$$\psi(z,\ y = 0) = \psi(z,\ y = H) = 0; \tag{1.5}$$

the "adhesion" condition

$$u(z,\ y = 0) = u(z,\ y = H) = 0. \tag{1.6}$$

Boundary conditions of the first and second kind are used on the bottom and top wall for temperature, respectively:

$$\Theta(z,\ y = 0) = 0,\ \partial\Theta/\partial y(z,\ y = H) = -\mathrm{Pe}^*. \tag{1.7}$$

Periodic boundary conditions are assumed for u, ψ, and Θ with respect to z:

$$\psi(z = 0,\ y) = \psi(z = L,\ y),\ u(z = 0,\ y) = u(z = L,\ y),\ \Theta(z = 0,\ y) = \Theta(z,\ = L,\ y). \tag{1.8}$$

It is clear from the formulation of the problem that transverse motion in the proposed model does not depend on the longitudinal motion, and no energy is transferred from the mean motion u to transverse pulsations w and v. Since dissipative terms are also absent from the equations for w and v, kinetic energy is conserved in the y–z plane.

In an actual flow, the rate of transverse motion always depends on the rate of longitudinal motion, so that it is necessary for these rates to agree. In our case, the mean rate

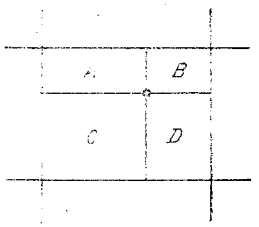

Fig. 1

of motion is determined by the parameter Re* (or v*), while the rates of transverse motions are determined by the quantities Γ_i (i = 1, ..., N). It is necessary to select Γ_i such that both ratios w/v* and v/v* are close to unity, as was seen in the experiment in [5]. Thus, Γ_i is a free parameter in the given model.

The energy of transverse motion is expressed by the integral

$$E = \frac{1}{2}\int\int_S (w^2 + v)^2 dydz. \tag{1.9}$$

In turn, the energy of the vortex system in the case of triviality of the total intensity of the vortices $\left(\sum_{i=1}^{N}\Gamma_i = 0\right)$ and a sufficiently uniform spatial distribution is determined by the formula [6]

$$E = \frac{1}{2} N\Gamma^2. \tag{1.10}$$

It follows from (1.9) and (1.10) that the intensity of point vortices for satisfaction of the conditions w ~ v* and v ~ v* must be taken in the form $\Gamma_i = v^*\sqrt{S/N}$, where S = HL is the cross-sectional area of the channel.

It is known that problems involving direct numerical modeling of turbulence face the challenge of not only having resolvable scales, but also of obtaining enough statistical data to find mean values [7].

This is connected with the fact that the statistical error in averaging decreases in inverse proportion to the root of the number of independent values of the random variable. Thus, to calculate mean values of the quantities which are of interest to us, it is necessary to use very large samples. This means that it is necessary to repeatedly integrate the equations over long time intervals with variation of the initial conditions (averaging over the ensemble of realizations). The problem is simplified in the case of uniform and stationary turbulence, since then we can average not only over time, but also over a uniform and stationary able (such as the coordinate z). All of the mean values will then be determined by the formula

$$\bar{u} = \frac{1}{(t_2 - t_1)L}\int_0^L\int_{t_1}^{t_2} u dt dz,$$

where $t_2 - t_1$ and L is the length of the time and space intervals, respectively.

Averaging over time was done with a steady flow, i.e., a statistically stationary flow, while the length of the interval was chosen to be much greater than the characteristic time of rotation of the vortices L/v* to obtain a reliable average.

2. Method of Solution. The problem of the motion of point vortices in an ideal fluid was solved by the method in [8]. This is essentially the Lagrange–Euler method of particles in cells, but instead of particles of mass we are examining point vortices. The solution was begun by determining the grid function ω in the right side of Eq. (1.1). The known position of the vortices was used to distribute the vorticity of each vortex among the four closest nodes of the grid in proportion to the four areas A, B, C, and D into which the grid cell was divided by lines passing through the vortex (Fig. 1). This method assures second-order accuracy and is called the method of weighted areas [8]. We then solved the Poisson equation

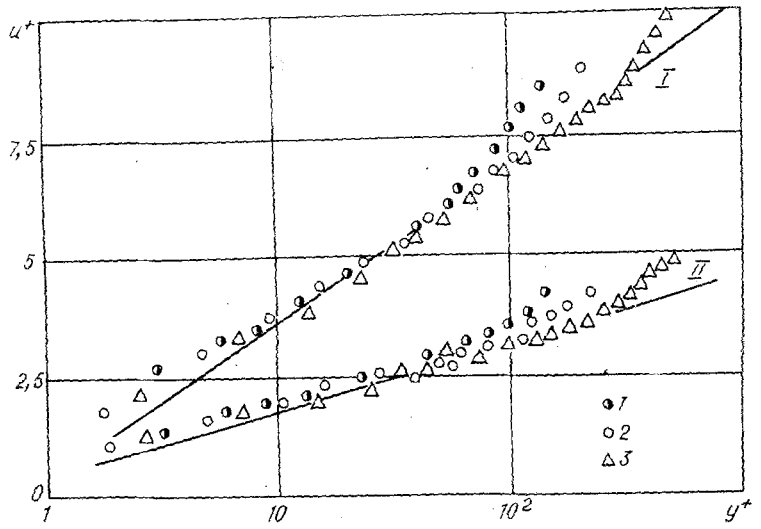

Fig. 2

(1.1) and used the already-known stream function and the operation of differentiation to determine the transverse velocity field v and w. We then used v and w to solve convection equations (1.2) and (1.3) and find the new position of the vortices. Time integration of system (1.1)-(1.3) was effected in the above sequence. The initial position of the vortices was randomly assigned. The total vorticity of the positive vortices was equal to the vorticity of the negative vortices. Equations (1.1)-(1.3) were approximated by second-order difference schemes on a nonuniform grid along the y axis, with crowding toward the walls. The grid was introduced in the direction away from the wall in accordance with a law of arithmetic progression from 0.1 to 1.6. At least 7-8 nodes were located in the region of the logarithmic layer. Altogether we studied 35 y nodes, so that the width $H \approx 30.6$.

Direct methods [9] are the most efficient methods of solving the Poisson equation (1.1) with right side (1.4) in a channel with boundary conditions (1.5)-(1.8). Fourier transformation in the z direction ensures periodicity of the solution with the period L over z and reduces the two-dimensional problem to a series of one-dimensional problems which are easily solved by a trial run over y [9]. We used a rapid Fourier transform (RFT) on a grid which was uniform with respect to z. The grid had 64 nodes and the period $L = 64$. The equations of motion of the vortices $\dot{x} = u_n$ $(n = 1, \ldots, N)$ were integrated by the second-order Eulerian method. The number of vortices in the calculations $N = 1024$.

Equations (1.2) and (1.3) were solved by implicit methods with the use of RFT for the variable z and a trial run for the variable y. The nonlinear terms were approximated by an explicit scheme similar to that of Arakav [10] and having the property of retaining the mean values of vorticity, the square of the curl, and kinetic energy. This makes it possible to transform the flow structure without distortion (the kinetic energy and the square of the curl are transferred from one grid node to another in the two-dimensional region without a hypothetical increase or decrease), which is important for integrating transport equations over a long time interval. We also used the usual central finite-difference scheme on the nonuniform grid.

Methodological work was done to determine the effect of errors of the approximation. The method of "sample" functions [10] was used to study the effect of the mesh of the grid, the time step, and the value of the coefficient in front of the diffusion term on the accuracy of the calculations. To do this, we used different grids which were nonuniform and uniform with respect to y. To check the accuracy of calculation of vortex motion in a plane, we compared the solutions for two point vortices obtained by Christiansen's method and solutions found analytically by the accurate method of conformal mapping [11]. The difference in the trajectories of the vortices calculated by these methods was no greater than 3% for the period of motion. The methodological study allowed us to guarantee that the error of the calculations for the parameters Re^* and Pe^* did not exceed 10^3 on a 65×35 grid.

The calculations were performed in two stages. In the first stage we calculated the motion of the vortices and on magnetic computer tape recorded successive (in time) values of the stream functions $\psi(z, y, t)$. The second stage entailed the solution of evolutionary

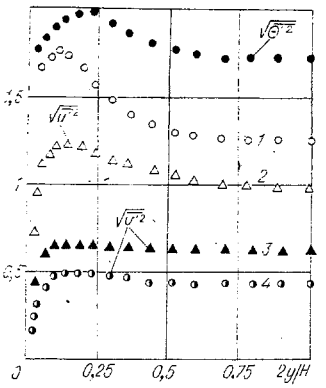

Fig. 3

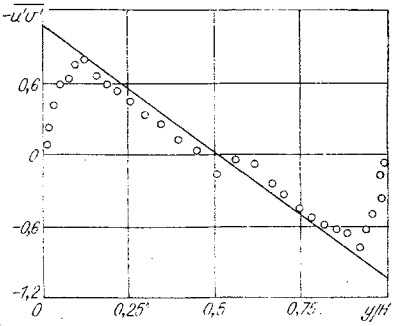

Fig. 4

equations of convective transport for u and Θ. Here we used the recorded values of the stream functions. The instantaneous values of $u(y, z, t)$ and $\Theta(y, z, t)$ were again recorded on magnetic tape for later statistical analysis in which we first calculated the mean values $\bar{\Theta}$ and $\bar{u}$ and then calculated the rms values $\sqrt{\overline{u'^2}}$, $\sqrt{\overline{\Theta'^2}}$, $\sqrt{\overline{v'^2}}$ and correlations $\overline{u'v'}$ and $\overline{v'\Theta'}$. The number of time steps was 2000, and the time step was $5\cdot10^{-2}$, so that the dimensionless computing time was 10^2.

3. Results of Calculations. We will present the most important results of modeling of turbulent transport. Curve I (Fig. 2) uses traditional semilogarithmic coordinates to show the velocity profile for $Re^* = 300$, 500, and 800 (points 1-3), which corresponds to flow-rate Reynolds numbers of 2030, 3615, and 5894. It is quite evident that the logarithmic section of the velocity profile stretches out with an increase in Re^*. The circulation of the point vortices Γ_i, which determines the rate of transverse motion, was chosen uniquely for this case. The logarithmic line of mean velocity has the form $u^+ = A \ln y^+ + B$, where $A = 1.41$ and $B = 0.35$, while $y^+ = Re^* y/H$.

Curve II is the profile of mean velocity for $\Gamma_i = 5$. It is apparent that longitudinal velocity decreases as a result of an increase in transverse velocity. Here, $A = 0.54$ and $B = 0.4$. It follows from Fig. 2 that the calculated mean velocity is considerably lower on the graph than the well-known experimental velocity profile in a channel in [5]. This is evidently attributable to the greater transverse velocity near the channel walls: due to the absence of viscosity, the motion is not damped by the wall (for example, the w component on the wall is generally nontrivial). Analogously to this, the greater turbulence in flows near a rough surface leads to a decrease in longitudinal velocity relative to the universal profile for a smooth wall. It can also be concluded from Fig. 2 that higher transverse velocity leads as it were to degeneration of the viscous sublayer; there is no section of linear behavior along y near the wall. At large y^+ in the central part of the channel, the velocity profiles deviate upward from the logarithmic law. The same is seen for the universal profile in the experiments in [5].

Figure 3 shows the rms pulsations of velocity and temperature: points 1 and 4 are for $\Gamma_i = 1$ and 2, and point 3 is for $\Gamma_i = 5$. The behavior of the theoretical longitudinal rms velocity pulsation is in qualitative agreement with the experimentally determined value [5]. The value for $\sqrt{\overline{v'^2}}$ is somewhat lower than the experimental value. Figure 4 shows the Reynolds stresses $\overline{u'v'}$ (the lines represent the total shear stresses). The temperature profile is shown in Fig. 5 for $\Gamma_i = 1$ and for $Pe^* = 300$, 500, and 800 (points 1-3). It is evident that it also has a logarithmic section. The formula for the mean temperature $\Theta^* = A_\Theta \ln y_- + B_\Theta$, where the constants $A_\Theta = 1.40$ and $B_\Theta = 3.35$; $y_- = Pe^* y/H$. The turbulent Prandtl number turns out to be very close to unity $Pr_t = A/A_\Theta = 1.41/1.40$. Figure 6 shows the turbulent heat flux $\overline{\Theta'v'}$.

The processor time required on a 1060 computer on one time step to solve the vortex-motion problem is 2.1 sec, while 1.5 sec are required to solve the convective transport equation. The maximum number of vortices in the computations was 10^4. The computing time here increases significantly (to 7 sec per step). The results of the calculations are not presented here, but it must be noted that the resulting mean values are smoother functions of y.

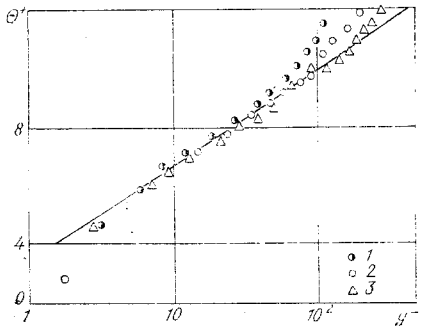

Fig. 5

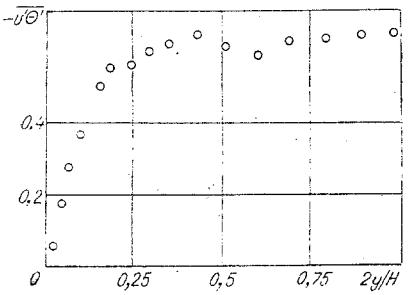

Fig. 6

Thus, we did not consider the effects of viscosity on turbulent transfer, but the most important theoretical characteristics of turbulent flow agree qualitatively with the experimental findings. It can be concluded that point vortices correctly describe the dynamics of large-scale energy-containing motions not directly dependent on viscosity. This means that the proposed model correctly describes not only mean characteristics, but also other statistical characteristics which are independent of viscosity – primarily second-order moments (pulsation intensity, Reynolds stresses, turbulent heat fluxes).

LITERATURE CITED

1. S. A. Orszag and A. T. Patera, "Calculation of von Karman's constant for turbulent channel flow," Phys. Rev. Lett., 47, No. 12 (1981).
2. A. Leonard, "Turbulent structures in wall-bounded shear flows observed via three-dimensional numerical simulations," in: Lecture Notes in Physics, Vol. 126, Springer-Verlag, Berlin (1981).
3. A. A. Townsend, The Structure of Turbulent Shear Flow, 2nd edn., Cambridge Univ. Press (1975).
4. E. D. Siggia and H. Aref, "Point-vortex simulation of the inverse energy cascade in two-dimensional turbulence," Phys. Fluids, 24, No. 1 (1981).
5. A. S. Monin and A. M. Yaglom, Statistical Hydromechanics, Vol. 1 [in Russian], Nauka, Moscow (1965).
6. Y. B. Pointin and T. S. Lundgren, "Statistical mechanics of two-dimensional vortices in a bounded container," Phys. Fluids, 19, No. 10 (1976).
7. W. Schumann, G. Gretzbach, and L. Clauser, "Direct methods of numerical modeling turbulent flows," in: Methods of Calculating Turbulent Flows [Russian translation], Mir, Moscow (1984).
8. J. P. Christiansen, "Numerical simulation of hydrodynamics by the method of point vortices," J. Comput. Phys., 13, No. 1 (1973).
9. A. L. Samarskii and E. S. Nikolaev, Methods of Solving Grid Equations [in Russian], Nauka, Moscow (1978).
10. P. J. Roache, Computational Fluid Dynamics, Hermosa (1976).
11. P. I. Geshev and B. S. Ezdin, "Motion of a vortex pair between parallel walls," Zh. Prikl. Mekh. Tekh. Fiz., No. 5 (1983).